Advances in Atmospheric Sciences

Impact Factor: 3.158

E-alert

ISSN 0256-1530
CN 11-1925/O4

Homogenised Monthly and Daily Temperature and Precipitation Time Series in China and Greece since 1960

Athanassios A. ARGIRIOU, Zhen LI, Vasileios ARMAOS, Anna MAMARA, Yingling SHI, Zhongwei YAN

Citation: Argiriou, A. A., Z. Li, V. Armaos, A. Mamara, Y. L. Shi, and Z. W. Yan 2023: Homogenised Monthly and Daily Temperature and Precipitation Time Series in China and Greece since 1960, *Adv. Atmos. Sci.*, 40, 1326–1336. doi: 10.1007/s00376-022-2246-4.

View online: https://doi.org/10.1007/s00376-022-2246-4

ADVANCES IN ATMOSPHERIC SCIENCES, VOL. 40, JULY 2023, 1326–1336

• Data Description Article •

Homogenised Monthly and Daily Temperature and Precipitation Time Series in China and Greece since 1960

Athanassios A. ARGIRIOU*[1], Zhen LI[2], Vasileios ARMAOS[1], Anna MAMARA[1,3], Yingling SHI[4], and Zhongwei YAN*[2,5]

[1]*Laboratory of Atmospheric Physics*, *Department of Physics*, *University of Patras*, *Rio* 26504, *Greece*

[2]*Key Laboratory of Regional Climate-Environment in Temperate East Asia*, *Institute of Atmospheric Physics*, *Chinese Academy of Sciences*, *Beijing* 100029, *China*

[3]*Hellenic National Meteorological Service*, *Athens* 16777, *Greece*

[4]*Longyang District Meteorological Service*, *Baoshan* 678007, *China*

[5]*College of Earth and Planetary Sciences*, *University of Chinese Academy of Sciences*, *Beijing* 100049, *China*

(Received 12 September 2022; revised 30 November 2022; accepted 20 December 2022)

ABSTRACT

In this paper, we describe and analyze two datasets entitled "Homogenised monthly and daily temperature and precipitation time series in China during 1960–2021" and "Homogenised monthly and daily temperature and precipitation time series in Greece during 1960–2010". These datasets provide the homogenised monthly and daily mean (TG), minimum (TN), and maximum (TX) temperature and precipitation (RR) records since 1960 at 366 stations in China and 56 stations in Greece. The datasets are available at the Science Data Bank repository and can be downloaded from https://doi.org/10.57760/sciencedb.01731 and https://doi.org/10.57760/sciencedb.01720. For China, the regional mean annual TG, TX, TN, and RR series during 1960–2021 showed significant warming or increasing trends of 0.27°C (10 yr)$^{-1}$, 0.22°C (10 yr)$^{-1}$, 0.35°C (10 yr)$^{-1}$, and 6.81 mm (10 yr)$^{-1}$, respectively. Most of the seasonal series revealed trends significant at the 0.05 level, except for the spring, summer, and autumn RR series. For Greece, there were increasing trends of 0.09°C (10 yr)$^{-1}$, 0.08°C (10 yr)$^{-1}$, and 0.11°C (10 yr)$^{-1}$ for the annual TG, TX, and TN series, respectively, while a decreasing trend of –23.35 mm (10 yr)$^{-1}$ was present for RR. The seasonal trends showed a significant warming rate for summer, but no significant changes were noted for spring (except for TN), autumn, and winter. For RR, only the winter time series displayed a statistically significant and robust trend [–15.82 mm (10 yr)$^{-1}$]. The final homogenised temperature and precipitation time series for both China and Greece provide a better representation of the large-scale pattern of climate change over the past decades and provide a quality information source for climatological analyses.

Key words: daily and monthly, temperature, precipitation, homogenisation, climate time series, Greece, China

Citation: Argiriou, A. A., Z. Li, V. Armaos, A. Mamara, Y. L. Shi, and Z. W. Yan, 2023: Homogenised monthly and daily temperature and precipitation time series in China and Greece since 1960. *Adv. Atmos. Sci.*, **40**(7), 1326–1336, https://doi.org/10.1007/s00376-022-2246-4.

Dataset Profile A	
Dataset title	Homogenised monthly and daily temperature and precipitation time series in China during 1960–2021
Time range	1960–2021
Geographical scope	China
Data format	".xlsx" and ".csv"
Data volume	536 MB
Data service system	https://doi.org/10.57760/sciencedb.01731 CSTR:31253.11.sciencedb.01731 DOI:10.57760/sciencedb.01731

* Corresponding authors: Athanassios A. ARGIRIOU, Zhongwei YAN
Emails: athanarg@upatras.gr, yzw@tea.ac.cn

(Continued.)

Dataset Profile A	
Sources of Funding	National Key Technologies Research and Development Program "Comparative study of changing climate extremes between China and Europe/Greece based on homogenised daily observations" (Grant No. 2017YFE0133600) The Hellenic and Chinese Governments, in the frame of the Greek – Chinese R & T Cooperation Programme project "Comparative study of extreme climate indices in China and Europe/Greece, based on homogenised daily observations – CLIMEX"(Grant No. Contract T7ΔKI-00046)
Dataset composition	In this dataset, there is an .xlsx file named Information at 366 stations in Greece, including four columns (No., Station No., Longitude, and Latitude), and four folders named RR, TG, TN, and TX. In each folder, there are two sub-folders named daily and monthly. In each subfolder, there are 366 .csv files named by station number. In each .csv file, there are two columns, i.e., date and records during 1960–2021.

Dataset Profile B	
Dataset title	Homogenised monthly and daily temperature and precipitation time series in Greece during 1960–2010
Time range	1960–2010
Geographical scope	Greece
Data format	".xlsx" and ".csv"
Data volume	67.5 MB
Data service system	https://doi.org/10.57760/sciencedb.01720 CSTR: 31253.11.sciencedb.01720 DOI: 10.57760/sciencedb.01720
Sources of Funding	The Hellenic and Chinese Governments, in the frame of the Greek – Chinese R & T Cooperation Programme project "Comparative study of extreme climate indices in China and Europe/Greece, based on homogenised daily observations – CLIMEX" (Grant No. Contract T7ΔKI-00046) National Key Technologies Research and Development Program "Comparative study of changing climate extremes between China and Europe/Greece based on homogenised daily observations " (Grant No. 2017YFE0133600)
Dataset composition	In this dataset, there is an .xlsx file named Information at 56 stations in Greece, including four columns (No., Station No., Longitude, and Latitude), and four folders named RR, TG, TN, and TX. In each folder, there are two sub-folders named daily and monthly. In each subfolder, there are 56 .csv files named by station No. In each .csv file, there are two columns, i.e., date and records during 1960–2010.

1. Introduction

There is a current consensus among the scientific community that a successful analysis of meteorological parameters to detect climate change requires reliable, long-term time series of good quality. The reliability of these time series strongly depends on both their quality and homogeneity. A climate time series is defined as homogeneous when its variations are solely due to the effects of weather and climate (Peterson et al., 1998). In practice, most weather data time series are affected by non-climatic factors such as station relocations, changes in the instrumentation and recalibrations, changes in the formulations used to calculate the mean temperature, changes in observation practices, etc. (Peterson et al., 1998), so their variations can potentially mask the actual climate change. Furthermore, the magnitude of these non-climatic biases is quite often equally as large as the variation of climate signals we attempt to detect (Della-Marta et al., 2004), and their cumulative impact may lead to incorrect conclusions. Therefore, the World Meteorological Organization (WMO) has issued guidelines and recommends that "No climate time series should be used without homogenisation testing and adjustment, where appropriate, and all National Meteorological and Hydrological Services and climate data providers that create and deliver climate datasets should routinely conduct homogenisation "(WMO, 2020).

Greece, located in eastern Europe, is an important node of the ancient Silk Road connecting China to Central Asia and Europe. Obviously, there are different climate regimes between the two countries, as well as different responses in extreme climate events due to global warming. As two key climatic factors, temperature and precipitation are of primary importance for weather and climate studies. Therefore, it is urgent to establish a reliable, long-term homogenised daily temperature and precipitation time series for the two countries, to effectively improve the database required for studying extreme weather and climate change in these two key nodes of the ancient Silk Road.

A variety of methods, such as Multiple Analysis of Series for Homogenisation (MASH) (Szentimrey, 1999), Climatol (Guijarro, 2021), and RHtest (Wang et al., 2007; Wang, 2008), have been applied to detect and adjust inhomogeneities in temperature and precipitation time series. Also, many homogenised climate datasets for different regions have already been produced, based on different methods (Cao et al., 2017; Li et al., 2018), undoubtedly improving the available data used for climate change studies. However, there are inevitable differences among these homogenised datasets, and this may complicate which one is deemed most suitable for climatological studies. Improved homogenisation results are expected if a second round of homogenisation is applied using a different method. This practice is recommended by the WMO (WMO, 2020) and followed by several researchers [e.g., Mamara et al. (2013) and, more recently, Coscarelli et al. (2021)].

In this paper, we present homogenised monthly and daily time series of the mean (TG), minimum (TN), and maximum (TX) temperature and precipitation (RR) for China and Greece dating back to 1960. These parameters have been selected with the intent of comparatively studying the variation of extreme climate indices in those two countries and the differences in their climate. For ease of use, detailed information about these two datasets is provided, and the effects of their inhomogeneities are estimated to help understand those differences that arise from different homogenisation methods. Finally, the long-term linear trends of climate change are assessed in the two countries.

The remainder of this paper is organized as follows. Section 2 describes the data records and the homogenisation methods. Section 3 demonstrates the effects of inhomogeneities on the long-term trends and their associated spatial patterns by comparing the raw data with the homogenised data. Section 4 presents the long-term trends of the regional mean annual and seasonal time series in China and Greece since 1960. Finally, section 5 summarizes the results.

2. Data and methods

2.1. *Data*

Raw daily TN, TG, TX, and RR data records for the period 1960–2021 at 366 stations in China were collected from the China Meteorological Administration, and analogous data records for a similar period of 1960–2010 at 56 stations in Greece were provided by the Hellenic National Meteorological Service. The above datasets were subjected to quality control according to the WMO guidelines (WMO, 2021). A monthly temperature value is the arithmetic average of the daily values of this month if there are no more than ten missing days in the month, among which no more than four are consecutive (5/11 rule). Monthly precipitation is defined as the sum of the daily precipitation for the month if there are no missing daily values for the month (WMO, 2017). Figure 1 shows the geographical distribution of the Chinese and Greek meteorological stations used in this study.

2.2. *Homogenisation methods*

The methods and the corresponding software used for homogenisation were Climatol (Guijarro, 2021) and MASH (Szentimrey, 1999, 2006, 2020). The Hellenic data were subjected to a first round of homogenisation by the Laboratory of Atmospheric Physics group using Climatol and then to a second round by the Chinese Academy of Sciences group using MASH. The Chinese data were first homogenised using MASH and then subjected to a second round using Climatol by the Chinese and Hellenic teams, respectively.

2.2.1. *Climatol*

The Climatol software tool offers much flexibility in the homogenisation process, featuring several parameters that can be tuned according to the characteristics of the time series being processed. The process of fine-tuning these parameters is iterative and largely based on trial and error. The first step towards this process is always an exploratory run of Climatol (with no homogenisation occurring).

The exploratory step provides several useful insights, the most important being the distribution of anomalies from their expected value and the values of the Standard Normal Homogeneity Test (SNHT) (Alexandersson, 1986) when applied to both the whole time series and the stepped and overlapped temporal windows.

Based on the results of the exploratory run, we can assign some initial trial values to the Climatol parameters and attempt the first homogenisation. Then, using the homogenisation results, we can tweak these parameters and run the homogenisation process from the beginning. This is repeated until reasonable results are obtained. The Climatol parameters that we ended up tuning are shown in Table 1.

After extensive testing and cross-referencing with the available metadata, Tables 2 and 3 list the parameters that best homogenise the data while keeping the bias low for Greece and China, respectively.

2.2.2. *MASH*

The MASH method was developed at the Hungarian Meteorological Service (Szentimrey, 1999). It is a relative

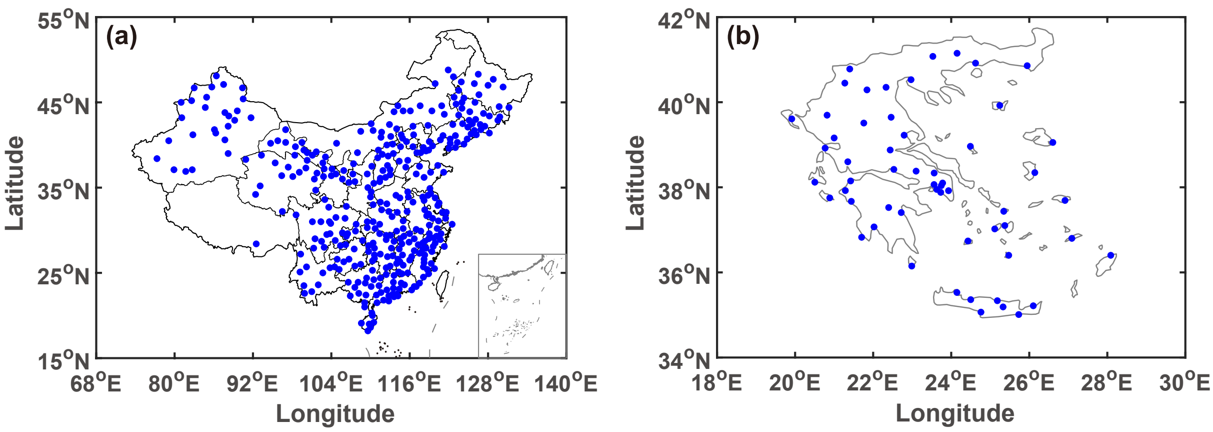

Fig. 1. Geographical distribution of the (a) 366 Chinese and (b) 56 Greek stations used to produce the homogenised time series.

Table 1. Tunned Climatol parameters.

Name	Function
snht1	Threshold value for the stepped SNHT window test.
snht2	Threshold value for the SNHT test when applied to the complete series.
std	Type of normalization. By default, std=3, the data will be standardized by subtracting the mean and dividing by the standard deviation, but if the variable has a natural zero (as is the case with precipitation), std=2 is preferable (data will be normalized just as ratios to the mean values). Another option is std=1, used only for applying differences to the mean values.
dz.max	Threshold of outlier tolerance. By default, anomalies greater than five standard deviations (of the anomaly series itself) will be rejected (conservative value).
wd	Distance (km) at which data will have half the weight of a station located at the same site of the series being estimated. The default values are 0 for the first two stages (meaning that all the reference data will have the same weight) and 100 for the last stage of missing data re-computation. The user can provide a vector of three values, one for each stage, as in wd = c(0, 200, 50).
swa	Size of the step forward to be applied to the windowed application of SNHT. The default value is 60, meaning that the test will be applied to the first 2 × 60 available terms of the series, and then this 120-term window will be skipped 60 terms forward for another test, and so forth until the end of the series is reached.

Table 2. Optimal Climatol parameters for the homogenisation of the Hellenic time series.

	TN	TG	TX	RR
snht1	50	27	35	17
snht2	55	37	45	18
Std	3	3	3	2
dz.max	6 (7)	6 (14)	6 (12)	6 (40)
Wd	Default	0, 100, 1000	0, 100, 1000	default
Swa	Default	default	default	24

Table 3. Optimal Climatol parameters for the homogenisation of the Chinese time series.

	TN	TG	TX	RR
snht1	50	50	50	26
snht2	90	90	90	45
std	3	3	3	2
dz.max	6 (11)	6 (8)	6 (7)	10 (40)
wd	Default	default	default	default
swa	Default	default	default	default

homogeneity test procedure that does not assume the reference series to be homogeneous. It consists of an iterative procedure designed to detect possible breakpoints through a mutual comparison with other climate data series within the same climatic area. The candidate series is selected among the available time series, and the remaining series are considered references. The role of each of the available series (candidate or reference) changes consecutively throughout the iterative procedure. A "good" reference series system can be produced through multiple comparisons between the candidate series and more reference series applied with different weighting factors. Several "difference" series are produced from the candidate and the weighted reference series. The optimal weighting is determined by minimizing the variance of the difference series to increase the efficiency of the statistical tests. Providing that the candidate series is the only common series among all the difference series, the breakpoints detected in all the difference series can be attributed to the candidate series. Version MASH v3.03 (Szentimrey, 2006) includes the following procedures: series comparison, breakpoint (change point) and outlier detection, correction of series, missing data completion, data quality control, automatic usage of metadata, and last but not least, a verification procedure to evaluate the homogenisation results.

In the present study, depending on the distribution of examined meteorological elements, the additive and multiplicative model of MASH v3.02 is applied to the daily temperature and precipitation series, respectively. The reference system of nine nearby stations for each candidate station is determined based on their distances to the candidate station. The significance level for testing breakpoints via the Monte Carlo method is $\alpha = 0.01$. The shifts or ratio values as well as the corresponding confidence intervals of breakpoints can also be obtained. The inhomogeneous sections are adjusted to the latest homogeneous part of the time series.

2.3. *Other methods*

The Mann-Kendall (MK) test (Mann, 1945; Kendall, 1975) and Theil-Sen estimator (Theil, 1950; Sen, 1968) are two non-parametric tests applied to time series trends and are mostly used by researchers in studying hydrological time series and climatic variations. The Theil-Sen estimator is more effective than the regression equation (Longobardi and Villani, 2010). In the present study, the Mann-Kendall test was applied at the 0.05 significance level for all the annual and seasonal temperature and precipitation series of

China and Greece to check whether these data exhibit an increasing or a decreasing trend. The Theil-Sen estimator is also employed to reveal eventual linear patterns and identify the trend magnitudes.

3. Inhomogeneities and effects on climate change

3.1. *Number of inhomogeneous stations*

To obtain a rough idea about how many stations are inhomogeneous and how these stations may influence the estimates of climate trends, Fig. 2a shows the number of inhomogeneous annual TG, TX, TN, and RR time series, ones with larger shifts detected by MASH, and ones further detected as inhomogeneous by CLIMATOL at 366 stations in China during 1960–2021. The results show there are 288, 240, 335, and 52 stations in the annual TG, TX, TN, and RR time series that were detected to be inhomogeneous via MASH, accounting for 78.7%, 65.6%, 91.5%, and 14.2% of the total stations, respectively. Clearly, there were more stations with an inhomogeneous temperature series than with an inhomogeneous precipitation series. To further characterize the impact of meaningful inhomogeneity on temperature or precipitation series and climate change, the stations with breakpoints which have a larger magnitude of shifts or ratios in the annual series, i.e., larger than 0.2°C or smaller than –0.2°C for temperature and larger than 1.2 or smaller than 0.8 for precipitation (ratio), are further defined as stations with greater inhomogeneity. For temperature, the estimated shift values that ranged from –0.2°C to 0.2°C occurred at 200, 194, and 213 stations (accounting for 54.64%, 53.01%, and 58.20% of total), and those larger than 0.2°C or smaller than –0.2°C occurred at 88, 48, and 122 stations (accounting for 24.04%, 13.11%, and 33.33% of the total) for TG, TX, and TN, respectively. For precipitation (ratio), the shifts for breakpoints ranged from 0.8 to 1.2 at most stations (accounting for 12.02% of the total), and those larger than 1.2 or less than 0.8 occurred at just eight stations (accounting for 2.19% of the total). Thus, it can be seen that the inhomogeneities detected by MASH had significant effects on a small number of stations, especially for the precipitation time series. Based on the detected breakpoints and estimated inhomogeneity by MASH and considering the actual climate change, the daily homogenised temperature and precipitation series were subjected to a second round of homogenisation using Climatol. Figure 2a reveals that the numbers of inhomogeneous stations additionally detected by CLIMATOL were limited, as only 9, 2, 27, and 1 stations for the TG, TX, TN, and RR series were further adjusted, respectively.

For Greece, to obtain a rough idea of how many stations are inhomogeneous and how they influence the estimates of climate trends, Fig. 2b gives the number of inhomogeneous annual TG, TX, TN, and RR series detected by Climatol and those further detected as inhomogeneous and ones with larger shift detected by MASH at 56 stations during 1960–2010. The results show that 35, 45, 30, and 10 stations in the annual TG, TX, TN, and RR series, were detected to be inhomogeneous using Climatol, which accounts for 62.50%, 80.36%, 53.57%, and 17.86% of the total stations, respectively. After this initial round of homogenisation, the data was homogenised again using MASH. Figure 2b reveals that 23, 25, 18, and 9 stations in the annual series are further detected to be inhomogeneous by MASH for TG, TX, TN, and RR; still, only 6, 6, 11, and 5 of them are detected to be of a larger shift caused by breakpoints, respectively.

3.2. *Effect of inhomogeneity on climate change*

3.2.1. *Temporal variation*

Furthermore, the temporal variation characteristics of the raw, MASH-based (Climatol-based), and the final homogenised [MASH + Climatol (Climatol + MASH)],

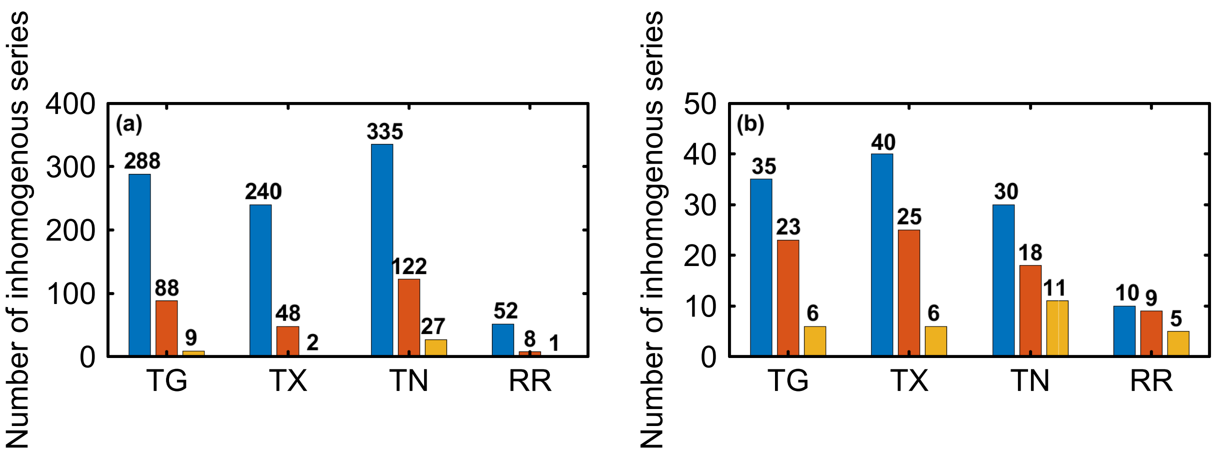

Fig. 2. (a) Number of stations in China with an inhomogeneous annual series (blue bars) and ones with larger shift (red bars) detected by MASH and those additionally detected as inhomogeneous by CLIMATOL (yellow bars) after the first round of homogenization; (b) Number of stations in Greece with an inhomogeneous annual series (blue bar) detected by Climatol, additional detected as inhomogeneous (red bar) and ones with larger shift (yellow bar) by MASH after the first round of homogenization.

regional mean annual temperature and precipitation series average over all stations in China (Greece) during 1960–2021 (1960–2010) are compared and analyzed. The interannual time series are shown in Fig. 3, and the corresponding regional mean long-term trends are listed in Table 4.

For China, both the MASH-based and the final homogenised annual TG, TX, TN, and RR series show consistent inter-annual variability against the raw data, with only slight differences (Figs. 3a1–3d1, left panel). Table 4 shows that the significant warming or increasing trend ($p< 0.05$) in regional mean annual TG, TX, TN, and RR series is 0.27°C $(10\ yr)^{-1}$, 0.22°C $(10\ yr)^{-1}$, 0.35°C $(10\ yr)^{-1}$, and 6.57 mm $(10\ yr)^{-1}$ based on MASH, 0.27°C $(10\ yr)^{-1}$, 0.22°C $(10\ yr)^{-1}$, 0.35°C $(10\ yr)^{-1}$, and 6.81 mm $(10\ yr)^{-1}$ based on the final homogenised series, slightly different from those based on the raw series [0.27°C $(10\ yr)^{-1}$, 0.23°C $(10\ yr)^{-1}$, 0.35°C $(10\ yr)^{-1}$, and 6.34 mm $(10\ yr)^{-1}$]. In terms of the series with larger shifts detected by MASH, as mentioned in the previous section, their mean TG, TX, TN, and RR series also show basically consistent trends between the raw [0.26°C $(10\ yr)^{-1}$, 0.20°C $(10\ yr)^{-1}$, 0.35°C $(10\ yr)^{-1}$, and 7.84 mm $(10\ yr)^{-1}$] and two homogenised results, especially for temperature. This demonstrates that the influence of homogenisation on estimating the large-scale mean climate trends in China is not very large because the effects of local inhomogeneities compensate for one another when calculating the averages. Meanwhile, the TN time series presents the largest warming

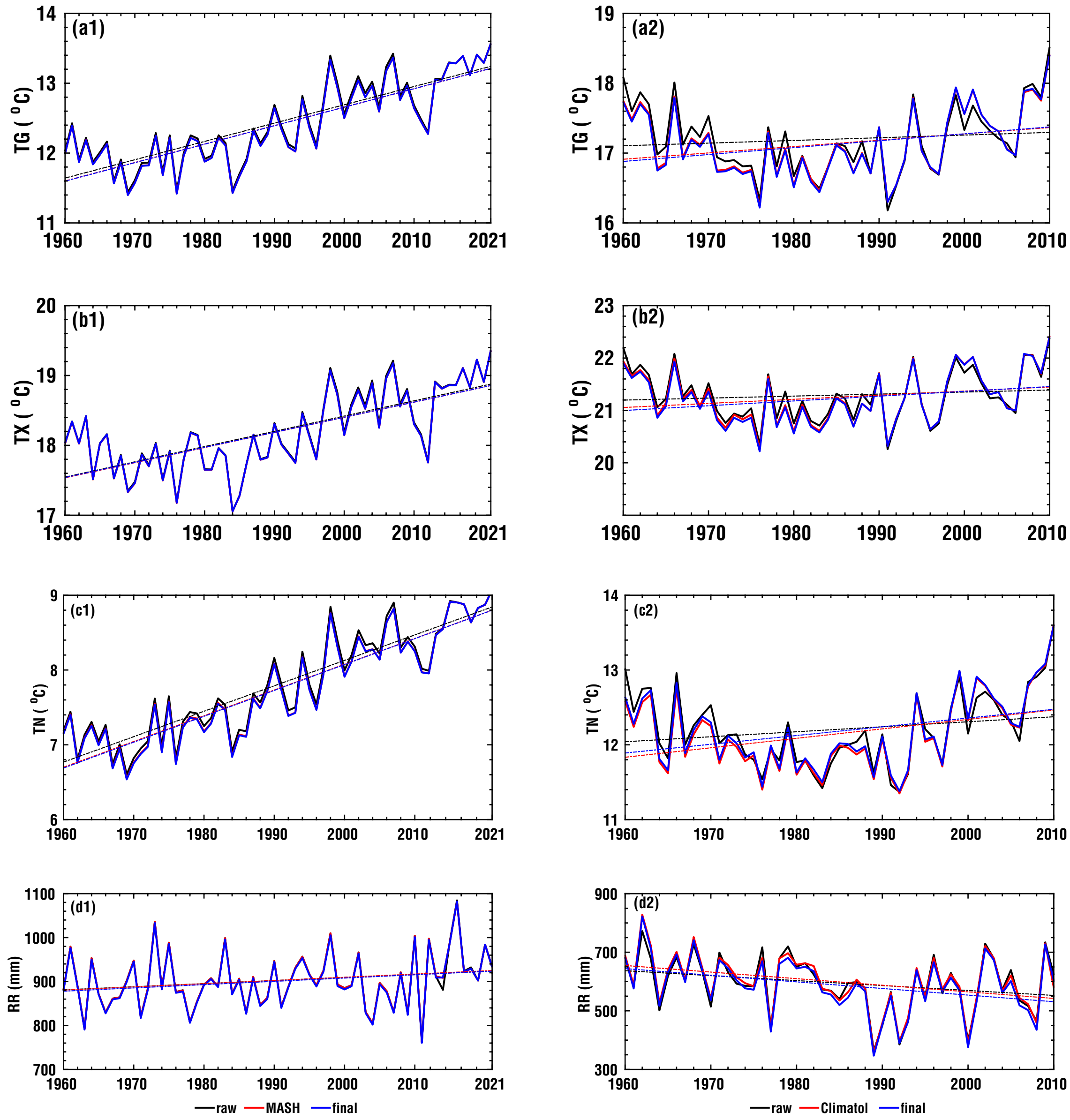

Fig. 3. Left panels: Regional mean annual TG, TX, TN, and RR series for China during 1960–2021 (black line: the raw data; red line: MASH-based homogenised data; blue line: final homogenised data). Right panels: same as left panels but for Greece during 1960–2010 (black line: the raw data; red line: Climatol-based homogenised data; blue line: final homogenised data).

Table 4. Trends of the averaged annual mean TG, TX, TN, and RR average for all series and ones with larger shifts estimated by MASH in the raw, MASH-based or Climatol-based, and final homogenised dataset in China during 1960–2021 and in Greece during 1960–2010.

	China						Greece					
	Regional mean series			Mean series of ones with larger shifts			Regional mean series			Mean series of ones with larger shifts		
	Raw	MASH-based	Final	Raw	MASH-based	Final	Raw	Climatol-based	Final	Raw	Climatol-based	Final
TG	0.27*	0.27*	0.27*	0.26*	0.28*	0.28*	0.02	0.08	0.09	0.13	0.1	0.12
TX	0.23*	0.22*	0.22*	0.20*	0.23*	0.23*	0.03	0.06	0.08	0.05	0.08	0.11*
TN	0.35*	0.35*	0.35*	0.35*	0.35*	0.36*	0.06	0.12*	0.11*	0.42*	0.09	0.08
RR	6.34	6.57*	6.81*	7.84*	7.84*	7.60*	–18.56*	–22.11*	–23.35*	8.72	–16.97	–18.03

* Trends that are significant at the 0.05 level according to the MK test. Units: °C (10 yr)$^{-1}$ for TG, TX, and TN; mm (10 yr)$^{-1}$ for RR.

rate, while the TX series presents the weakest warming rate for both the raw time series and the homogenised ones.

For Greece, compared with the raw data, both the Climatol based and the final homogenised annual TG, TX, TN, and RR series also show consistent inter-annual variability but with smaller differences (Fig. 3, right panel). The spatially averaged (over the whole country) annual TG, TX, TN, and RR series have trends of 0.09°C (10 yr)$^{-1}$, 0.08°C (10 yr)$^{-1}$, 0.11°C (10 yr)$^{-1}$, and –23.35 mm (10 yr)$^{-1}$ in the final homogenised time series. These trends are similar to those calculated with the time series homogenised only with Climatol but different from those calculated from the raw data, especially for precipitation. Table 4 also demonstrates that the largest warming rate is observed for the TN series, while the TX series has the lowest warming rate. This feature is consistent in both the Climatol-based and the final homogenised data. This behavior is also observed in the Chinese data. However, the differences in trends between the raw and two homogenised time series for series with larger shifts are of greater magnitude and cannot be ignored. A possible reason could be the missing records among the different time periods in these series, which, at least to some extent, enhance the interannual variability of the raw series. Clearly, the homogeneities or missing records in these raw local observations can overwhelm and even reverse the long-term trends, while the Climatol-based and final homogenised data provide the same-sign trends. Notably, although there are differences between the two homogenised results, the adjusted series generally improves the estimates of climatic trends.

3.2.2. *Geographical patterns*

To further reveal the impact of inhomogeneities on the spatial patterns of climate change, the spatial distribution of annual trends (Theil-Sen estimators) at all stations in the raw and homogenised data both in China and Greece are shown in Fig. 4. For China, compared with the MASH-based data and the final data, the raw data (Figs. 4a, d, g) exhibit unusually large warming trends in places or local negative trends at certain stations (mainly in southwestern areas), incoherently nested in the large-scale warming pattern. In contrast, warming trends tended to slow down and toward consistency with the surrounding large-scale change characteristics after the MASH-based adjustment (Figs. 4b, e, h). After further adjustment based on Climatol, the spatial distribution patterns were basically the same (Figs. 4c, f, i). The large-scale patterns of trends during the last 62 years in China were improved by both homogenised datasets and yielded better spatial consistency. The final homogenised data indicate that over 97% of stations prevailed with consistent warming trends in their annual TG, TX, and TN series. The warming trends of TG are above 0.10°C (10 yr)$^{-1}$ throughout all of China and were larger to the northwest of Xinjiang and in central-eastern parts of Inner Mongolia, whose warming trend was as large as 0.50°C (10 yr)$^{-1}$ (Fig. 4c). The TX series had larger warming trends in Northwest China [more than 0.30°C (10 yr)$^{-1}$] and weaker warming trends in South China about 0.10–0.25°C (10 yr)$^{-1}$ (Fig. 4f). In terms of TN, the warming trends were larger in Northwest China, North China, and Northeast China [more than 0.5°C (10 yr)$^{-1}$], while they were smaller in South China, Southwest China, and Central China about 0.3°C (10 yr)$^{-1}$. Generally, the warming trends in North China were greater than those in South China, and those of TN were significantly greater than in TX. For RR, 66.9% of stations showed an increasing trend. The trend patterns of the annual RR series, whether produced by MASH or the final time series, are consistent with the raw data. Annual precipitation series with increasing trends were observed in East China, South China, and the northeastern portion of Northwest China, while decreasing trends were mainly found in Southwest China (Fig. 4i).

To illustrate the spatial impact of inhomogeneities on climate change, the spatial distribution of significant annual trends in Greece is presented in Fig. 5. Impressively, the spatial consistency of trends in TG, TX, TN, and RR series in raw data is weak, and had improved significantly after the homogenisation by Climatol. After the second round of homogenisation using MASH, the spatial distribution patterns remained basically the same. The final data indicate that there were 56, 53, and 55 annual TG, TX, and TN series, respectively, showing positive trends that ranged between 0.04°C (10 yr)$^{-1}$ and 0.16°C (10 yr)$^{-1}$ for TG, –0.01°C (10 yr)$^{-1}$ to 0.19°C (10 yr)$^{-1}$ for TX, and –0.02°C (10 yr)$^{-1}$ to 0.22°C (10 yr)$^{-1}$ for TN. Generally, the warming trends of TN were significantly greater than those of TX. The warm-

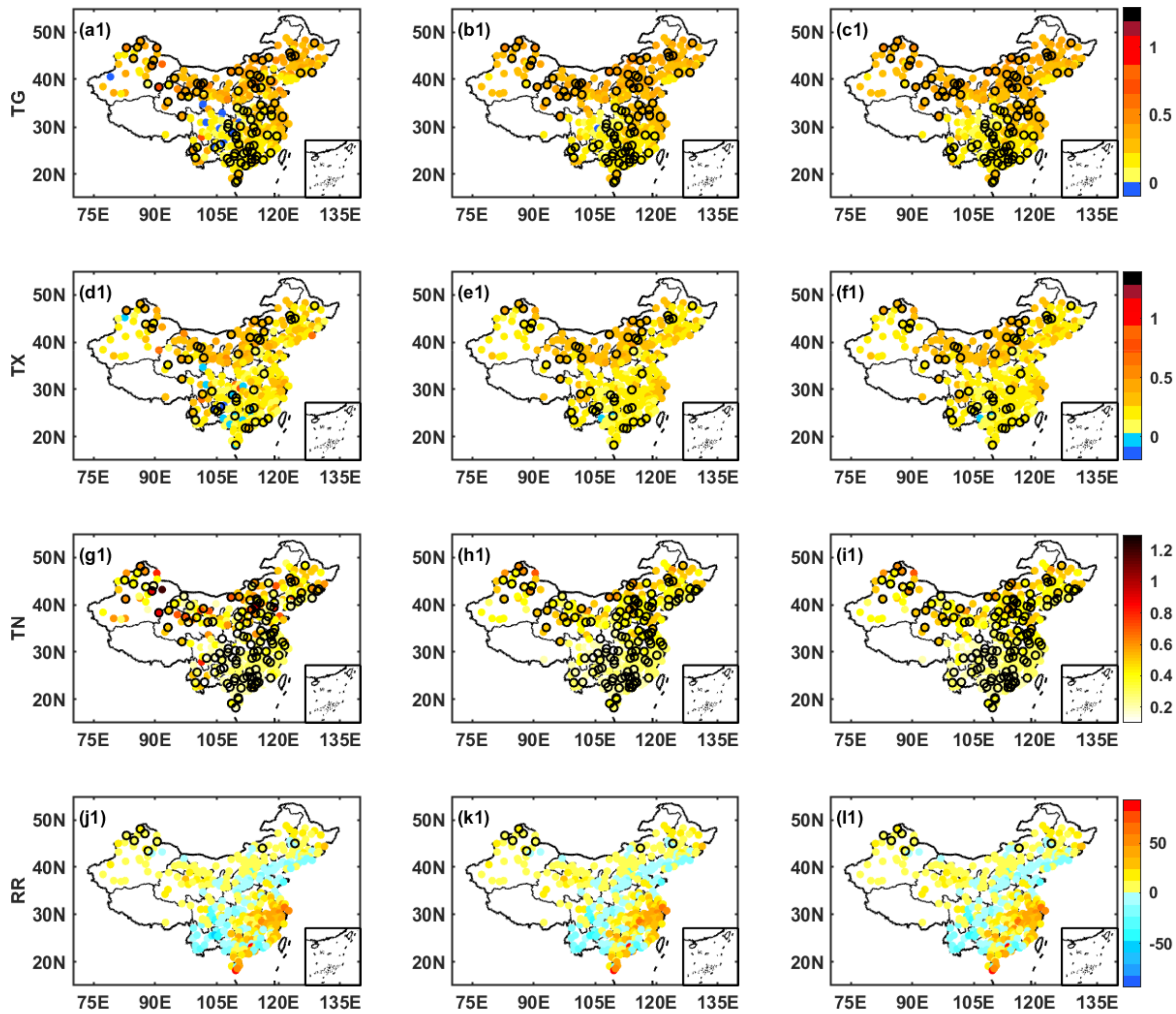

Fig. 4. Spatial distribution of linear trends in the annual TG, TX, TN, and RR series at 366 stations during 1960–2021 in China, compared between the raw (a, d, g, j), MASH-based (b, e, h, k), and final homogenised data (c, f, i, l). Dots with black circles denote series with larger shifts detected by MASH. Units: °C (10 yr)$^{-1}$ for TG, TX, and TN; mm (10 yr)$^{-1}$ for RR.

ing trends of the final homogenised time series for TG and TN appear to have a uniform spatial distribution. This is not the case for TX, where warming appears to be more significant in northern and eastern Greece. Regarding RR, the annual precipitation series at 51 stations show decreasing trends, and the strongest downward trends were observed in western Greece. Overall, there is a better spatial consistency of large-scale changing signals in temperature and precipitation after homogenisation.

Above all, the homogenised temperature and precipitation datasets improved the database for studying large-scale structures of climate changes not only for long-term temporal variation but also for the geographical patterns in both China and Greece.

4. Long-term climate changes over China and Greece since 1960

The seasonal and annual trends and their corresponding significance obtained from the final data at all stations in both countries are further assessed by the MK test and the Theil-Sen estimator. Figure 6 presents the percentage of stations with significant and non-significant trends in the final seasonal and annual series for 366 stations in China and 56 stations in Greece, according to the MK test.

For China, Fig. 6a reveals that significant warming trends prevail in seasonal and annual TG, TX, and TN series at over 80% of all stations, especially for the annual TG and in the autumn, winter, and annual TN series, which are up to 100%. There were no stations with significant negative trends in either the seasonal or annual series. On the contrary, seasonal (except for winter) and annual precipitation series show significant increasing trends for a limited number of stations (less than 20%). For regional mean temperatures, as mentioned in section 3.2.1, the annual TG, TX, and TN series covering the period 1960–2021 showed significant warming trends of about 0.27°C (10 yr)$^{-1}$, 0.22°C (10 yr)$^{-1}$, and 0.35°C (10 yr)$^{-1}$, respectively. For seasonal mean tem-

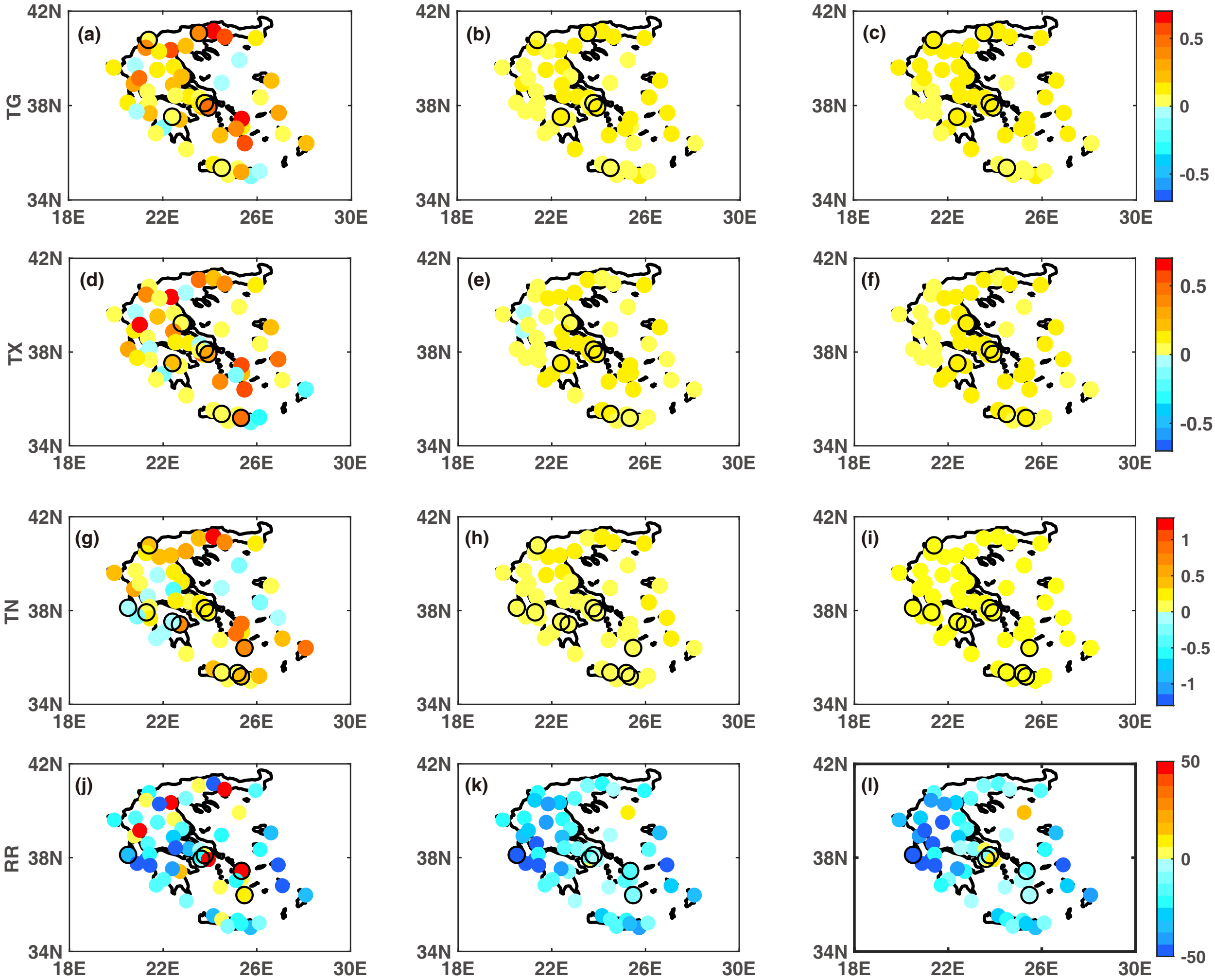

Fig. 5. Spatial distribution of linear trends in the annual TG, TX, TN, and RR series at 56 stations during 1960–2010 in Greece, compared between the raw (a, d, g), Climatol-based (b, e, h), and final homogenised data (c, f, i). Dots with black circles denote the series with larger shifts, as detected by MASH. Units: °C (10 yr)$^{-1}$ for TG, TX, and TN; mm (10 yr)$^{-1}$ for RR.

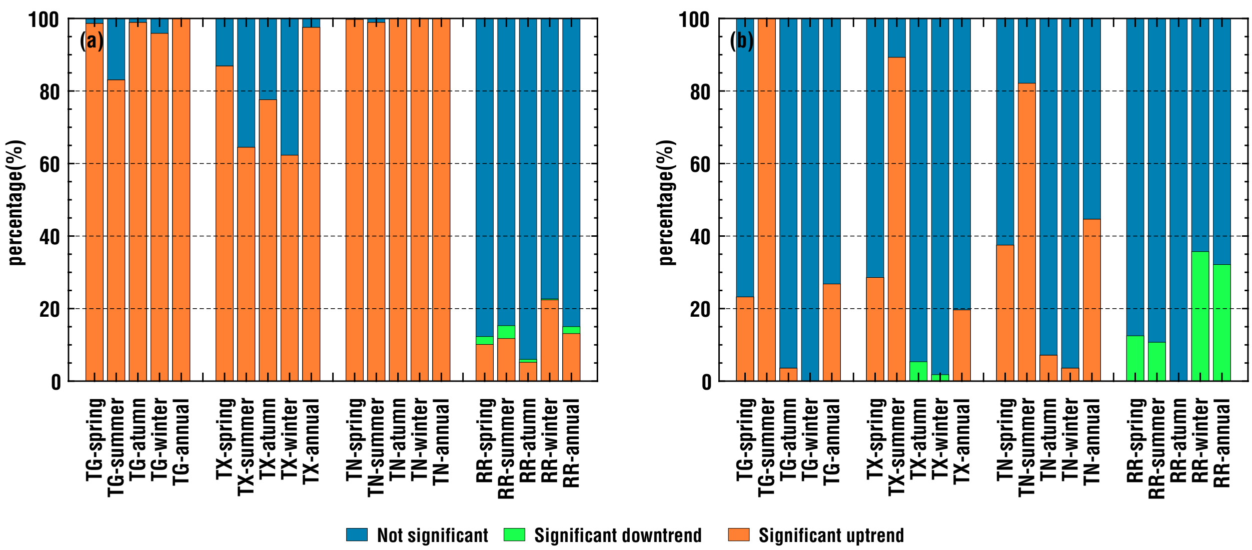

Fig. 6. Percentage of stations with significant and non-significant trends in their final seasonal and annual series at 366 stations in China (a) and at 56 stations in Greece (b) according to the MK test.

peratures, the fastest warming trends were up to 0.35°C (10 yr)$^{-1}$, 0.25°C (10 yr)$^{-1}$, and 0.44°C (10 yr)$^{-1}$ for the TG, TX, and TN series, respectively, and occurred in winter, followed by spring and autumn. The lowest trends of 0.18°C (10 yr)$^{-1}$, 0.14°C (10 yr)$^{-1}$, and 0.27°C (10 yr)$^{-1}$ occurred in summer (Table 5). For RR, the final homogenised data exhibited decreasing trends of –0.4 mm (10 yr)$^{-1}$ in spring and –0.60 mm (10 yr)$^{-1}$ in autumn, and increasing trends of 4.46 mm (10 yr)$^{-1}$ in summer, 2.46 mm (10 yr)$^{-1}$ in winter, and 6.81 mm (10 yr)$^{-1}$ annually for the period 1960–2021.

For Greece, Table 5 shows that the warming trends are only significant for the summer season, with no significant trends during spring, autumn, and winter. Figure 6b reveals that significant warming trends prevail in the summertime TG, TX, and TN series for more than 80% stations, especially for the summertime TG series, where the percentage reaches 100%. On the contrary, there are no significant trends in the temperature series for the autumn and winter season for most of the stations. For the trends in RR, 45, 24, 27, 54, and 51 stations in the spring, summer, autumn, winter, and annual series show decreasing trends, but the majority are not significant (less than 40% of total stations). For regional mean temperatures, the annual TG, TX, and TX series covering the period 1960–2010 show warming trends of 0.09°C (10 yr)$^{-1}$, 0.08°C (10 yr)$^{-1}$, and 0.11°C (10 yr)$^{-1}$, respectively. The highest warming trends were up to 0.29°C (10 yr)$^{-1}$, 0.29°C (10 yr)$^{-1}$, and 0.28°C (10 yr)$^{-1}$ per decade for the TG/TX/TN time series, respectively, and occurred in summer, closely followed by the spring trends, but these trends are markedly less in autumn and winter (Table 5). For RR, the final homogenised data show that all seasonal and annual series show decreasing trends of –4.47 mm (10 yr)$^{-1}$ in spring, –0.65 mm (10 yr)$^{-1}$ in summer, –0.04 mm (10 yr)$^{-1}$ in autumn, –15.82 mm (10 yr)$^{-1}$ in winter, and –23.35 mm (10 yr)$^{-1}$ in the annual temperature series of 1960–2010. Thus, it is clear that the long-term regional mean temperature and precipitation series present different temporal variation characteristics in China and Greece.

5. Summary

Differences in homogenised temperature and precipitation datasets based on different methods are an unavoidable problem in basic and applied meteorological science. In the present study, we first homogenised the daily TG, TX, TN, and RR series at 366 (56) stations in China (Greece) during 1960–2021 (1960–2010) by using the MASH (CLIMATOL) methods and then subjected them to a second round of homogenisation using CLIMATOL (MASH). In this way, we produced the final homogenised daily temperature and precipitation datasets for 1960 and beyond for both countries. The number of stations with an inhomogeneous time series and the effects of inhomogeneities on long-term trends on their spatial patterns were analyzed and compared among the raw, MASH-, Climatol- based data, and final homogenised data. Finally, the long-term regional mean seasonal and annual trends of the final data were assessed, beginning in 1960 over China and Greece. The main conclusions can be summarized as follows.

More inhomogeneous stations were found for the temperature series than the precipitation series. For China, 78.7%, 65.6%, 91.5%, and 14.2% out of a total of 366 stations in their raw monthly TG, TX, TN, and RR series were detected to be inhomogeneous via MASH, and only 9, 2, 27, and 1 stations were further adjusted by CLIMATOL, respectively. For the entirety of China, both the seasonal and annual TG, TX, and TN series indicate significant warming trends at over 80% of the stations. In comparison, significant increasing trends in the precipitation series are shown only at a limited number of stations (less than 20%) (except for winter). The annual TG, TX, and TN series averaged over China covering the period 1960–2021 show significant warming trends of about 0.27, 0.22, and 0.35°C per decade, respectively. The fastest warming trends occurred in winter, followed by spring and autumn, while the lowest occurred in summer. For the annual precipitation (RR), the spring and autumn series exhibit decreasing trends of –0.4 mm (10 yr)$^{-1}$ and –0.60 mm (10 yr)$^{-1}$, while the summer, winter, and annual series show increasing trends of 4.46 mm (10 yr)$^{-1}$, 2.46 mm (10 yr)$^{-1}$, and 6.81 mm (10 yr)$^{-1}$ during 1960–2021.

For Greece, 62.50%, 80.36%, 53.57%, and 17.86% of the annual TG, TX, TN, and RR time series during 1960–2010 were found to be inhomogeneous by Climatol, then 23, 25, 18, and 9 stations were further adjusted by MASH, and 6, 6, 11, and 5 of them were estimated with meaningful adjustments, respectively. The annual temperature series displayed a small warming trend of 0.09°C (10 yr)$^{-1}$,

Table 5. The trends of regional mean seasonal and annual temperature and precipitation series in China during 1960–2021 and in Greece during 1960–2010.

	China				Greece			
	TG	TX	TN	RR	TG	TX	TN	RR
Spring	0.32*	0.29*	0.37*	–0.40	0.14	0.16	0.13*	–4.47
summer	0.18*	0.14*	0.27*	4.46	0.29*	0.28*	0.28*	–0.65
Autumn	0.24*	0.19*	0.32*	–0.60	0.02	–0.06	0.09	–0.04
Winter	0.35*	0.25*	0.44*	2.46*	–0.02	0.00	0.00	–15.82*
Annual	0.27*	0.22*	0.35*	6.81*	0.09	0.08	0.11*	–23.35*

* Trends that are significant at the 0.05 level according to the MK test. Units: °C (10 yr)$^{-1}$ for TG, TX, and TN; mm (10 yr)$^{-1}$ for RR.

0.08°C (10 yr)$^{-1}$, and 0.11°C (10 yr)$^{-1}$ for TG, TX, and TN, respectively, but among these, only that of TN is statistically significant. Similarly, RR shows a statistically significant decreasing trend of –23.35 mm (10 yr)$^{-1}$. However, the seasonal trends show a different picture, with significant warming trends of –0.28°C (10 yr)$^{-1}$ and –0.29°C (10 yr)$^{-1}$ during summer and no significant trend for spring (except for TN), autumn, and winter for all temperature time series. Similarly, for precipitation, there was a strong decreasing trend of –15.82 mm (10 yr)$^{-1}$ for winter, with no significant trend for the other seasons.

These unique homogenised temperature and precipitation datasets are anticipated to be a sound base for studying regional climate change, especially for comparing weather and climate extremes between China, Greece, and other areas of southeastern Europe.

Acknowledgements. This work was funded by the Hellenic and Chinese Governments, in the frame of the Greek-Chinese R & T Cooperation Programme project "Comparative study of extreme climate indices in China and Europe/Greece, based on homogenised daily observations — CLIMEX" (Contract T7ΔKI-00046) and the National Key Technologies Research and Development Program "Comparative study of changing climate extremes between China and Europe/Greece based on homogenised daily observations" (Grant No. 2017YFE0133600).

REFERENCES

Alexandersson, H., 1986: A homogeneity test applied to precipitation data. *J. Climatol.*, **6**, 661−675, https://doi.org/10.1002/joc.3370060607.

Cao, L. J., Z. W. Yan, P. Zhao, Y. N. Zhu, Y. Yu, G. L. Tang, and P. Jones, 2017: Climatic warming in China during 1901-2015 based on an extended dataset of instrumental temperature records. *Environmental Research Letters*, **12**, 064005, https://doi.org/10.1088/1748-9326/aa68e8.

Coscarelli, R., G. N. Caroletti, M. Joelsson, E. Engström, and T. Caloiero, 2021: Validation metrics of homogenization techniques on artificially inhomogenized monthly temperature networks in Sweden and Slovenia (1950–2005). *Scientific Reports*, **11**, 18288, https://doi.org/10.1038/s41598-021-97685-7.

Della-Marta, P., D. Collins, and K. Braganza, 2004: Updating Australia's high-quality annual temperature dataset. *Aust. Meteor. Mag.*, **53**, 75−93.

Guijarro, J. A., 2021: Homogenisation of Climatic Series with Climatol: Version 3.1.1. [Available online from https://climatol.eu/homog_climatol-en.pdf]

Kendall, M. G., 1975: *Rank Correlation Methods*. Oxford University Press.

Li, Z., Z. W. Yan, L. J. Cao, and P. D. Jones, 2018: Further-adjusted long-term temperature series in China based on MASH. *Adv. Atmos. Sci.*, **35**(8), 909−917, https://doi.org/10.1007/s00376-018-7280-x.

Longobardi, A., and P. Villani, 2010: Trend Analysis of annual and seasonal rainfall time series in the Mediterranean area. *International Journal of Climatology*, **30**(10), 1538−1546, https://doi.org/10.1002/joc.2001.

Mamara, A., A. A. Argiriou, and M. Anadranistakis, 2013: Homogenization of mean monthly temperature time series of Greece. *International Journal of Climatology*, **33**, 2649−2666, https://doi.org/10.1002/joc.3614.

Mann, H. B., 1945: Nonparametric tests against trend. *Econometrica*, **13**, 245−259, https://doi.org/10.2307/1907187.

Peterson, T. C., and Coauthors, 1998: Homogeneity adjustments of *in situ* atmospheric climate data: a review. *International Journal of Climatology*, **18**, 1493−1517, https://doi.org/10.1002/(SICI)1097-0088(19981115)18:13<1493::AID-JOC329>3.0.CO;2-T.

Sen, P. K., 1968: Estimates of the regression coefficient based on Kendall's Tau. *Journal of the American Statistical Association*, **63**, 1379−1389, https://doi.org/10.1080/01621459.1968.10480934.

Szentimrey, T., 1999: Multiple analysis of series for homogenisation (MASH). *Proc. 2nd Seminar for Homogenisation of Surface Climatological Data*, Budapest, Hungary, WCDMP-No. 41, WMO, 27−46.

Szentimrey, T., 2006: Development of MASH homogenisation procedure for daily data. *Proc. 5th Seminar for Homogenization and Quality Control in Climatological Databases*, Budapest, Hungary, WCDMP-No. 71, WMO, 123−130.

Szentimrey, T., 2020: Mathematical questions of homogenization and summary of MASH. *Proc. 10th Seminar for Homogenization and Quality Control and 5th Conf. on Spatial Interpolation Techniques in Climatology and Meteorology*, Budapest, Hungary, WCDMP-No. 86, WMO, 4−17.

Theil, H., 1950: A rank-invariant method of linear and polynomial regression analysis I, II and III. *Proc. Kon. Ned. Akad. Wetensch. Ser. A,* **53**, 386−392, 521−525, 1397−1412.

Wang, X. L., 2008: Penalized maximal *F* test for detecting undocumented mean shift without trend change. *J. Atmos. Oceanic Technol.*, **25**, 368−384, https://doi.org/10.1175/2007JTECHA982.1.

Wang, X. L., Q. H. Wen, and Y. H. Wu, 2007: Penalized maximal *t* test for detecting undocumented mean change in climate data series. *J. Appl. Meteorol. Climatol.*, **46**, 916−931, https://doi.org/10.1175/JAM2504.1.

WMO, 2017: WMO guidelines on the calculation of climate normals. WMO/TD-No. 1203, 18 pp.

WMO, 2020: Guidelines on homogenisation. WMO/TD-No. 1245, 54 pp.

WMO, 2021: Guidelines on surface station data quality control and quality assurance for climate applications. WMO/TD-No. 1269, 43 pp.